PHILOSOPHICAL TRANSACTIONS OF THE ROYAL SOCIETY A
MATHEMATICAL, PHYSICAL & ENGINEERING SCIENCES

A new method to predict vessel/platform critical dynamics in a realistic seaway

S. Vishnubhotla, J. Falzarano and A. Vakakis

Phil. Trans. R. Soc. Lond. A 2000 **358**, 1967-1981
doi: 10.1098/rsta.2000.0623

THE ROYAL SOCIETY

A new method to predict vessel/platform critical dynamics in a realistic seaway

By S. Vishnubhotla[1], J. Falzarano[1] and A. Vakakis[2]

[1] *School of Naval Architecture and Marine Engineering, University of New Orleans, 911 Engineering Building, New Orleans, LA 70148, USA*

[2] *Department of Mechanical and Industrial Engineering, University of Illinois, IL 61801, USA*

In this paper, a recently developed approach is used that makes use of a closed form analytic solution, which is exact up to the first order of randomness, and takes into account exactly the unperturbed (no forcing or damping) global dynamics. The result of this is that very-large-amplitude nonlinear vessel motion in a random seaway can be analysed with techniques similar to those used to analyse nonlinear vessel motions in a regular (periodic) seaway; the practical result being that dynamic capsizing studies can be undertaken considering the true randomness of the design seaway. The capsize risk associated with operation in a given sea spectrum can be evaluated during the design stage or when an operating area change is being considered. Moreover, this technique can also be used to guide physical model tests or computer simulation studies to focus on critical vessel and environmental conditions which may result in dangerously large motion amplitudes. In order to demonstrate the practical usefulness of this approach, extensive comparative results are included. The results are in the form of solutions which lie in the stable or unstable manifolds and are then projected onto the phase plane.

Keywords: nonlinear ship/platform motions; stochastic vessel dynamics; critical ship/platform roll dynamics; nonlinear dynamical systems; phase plane

1. Introduction and background

Research studies of nonlinear ship and floating offshore platform rolling motion using dynamical systems' approaches have become quite common (Thompson 1997). However, practical ship design stability criteria still focus on the static restoring moment curve as the sole or dominant indicator of the vessel's resistance to capsizing and only consider the motion in an implicit or very approximate manner. Most nonlinear motions studies are limited to single-degree-of-freedom and regular-wave (periodic) excitation, with few exceptions (see, for example, Hsieh *et al*. 1993; Simiu & Frey 1996; Soliman & Thompson 1990; Lin & Yim 1995). It is well known that roll cannot always be decoupled from the other degrees of freedom, but more importantly it is well known that sea waves are not regular but are in fact random. It is common in the design of ships and floating offshore platforms to make narrow banded assumptions and predict short-term extremes using the Rayleigh probability density function (PDF) (see, for example, Ochi 1998). In this study, the highly nonlinear

near-capsizing behaviour of a small fishing vessel and a very large semi-submersible platform in a random seaway is analysed by using an analytical solution to the differential equation. The availability of such a closed form solution allows safe basin boundary curves for this pseudo-randomly forced system to be generated.

The *Patti-B* was a small fishing vessel which has the dubious distinction of having capsized twice. This vessel operated off the east coast of the United States and was involved in two capsizings. Initially, she capsized in shallow water and her owners salvaged her (NTSB 1979). The second time, the vessel capsized in deeper waters and all hands were lost.

The 'mobile offshore base' (MOB) is a structure, approximately one mile long, made up of three to five individual, large, semi-submersible single base units (SBUs). Transit draft has been identified as a particular area of concern from a dynamics and stability standpoint. Although while at operating draft, semi-submersibles are relatively transparent to wave excitation due to the majority of the hull volume being submerged far below the water surface, while at transit draft, an individual unconnected SBU operates essentially as a catamaran with a relatively high metacentric height. With the lower hulls penetrating the water surface, wave excitation can be important. Moreover, due to the reduced freeboard of the lower hulls, wetting of the their tops may also occur. This will result in a parametric excitation not explicitly considered herein.

2. Physical system modeling

The focus of this study is the highly nonlinear rolling motion of ships and floating offshore platforms, possibly leading to capsizing. For the small fishing vessel, the roll axis is the critical motion axis. Even though semi-submersibles generally have critical dynamics about a diagonal axis (Kota *et al*. 1997, 1998), due to the relatively large length-to-beam ratio of the MOB SBUs, roll is assumed to be critical for this analysis. Roll is, in general, coupled to the other degrees of freedom; however, under certain circumstances, it is possible to approximately decouple roll from the other degrees of freedom and to consider it in isolation. This allows focus on the critical roll dynamics. The decoupling is most valid for vessels which are approximately fore–aft symmetric; this eliminates the yaw coupling. The USNA generic MOB is exactly fore and aft symmetric. Moreover, by choosing an appropriate roll-centre coordinate system, the sway is approximately decoupled from the roll (Webster 1989). For ships, it has been shown in previous studies that even if the yaw and sway coupling are included, the results differ only in a quantitative sense. The yaw and sway act as passive coordinates and do not qualitatively affect the roll (Zhang & Falzarano 1994).

The other issue is the modelling of the fluid forces acting on the hull. Generally speaking, the fluid forces are subdivided into excitations and reactions (Newman 1982). The wave-exciting force is composed of one part due to incident waves and another due to the diffracted waves. These forces are strongly a function of the wavelength/frequency. The reactive forces are composed of hydrostatic (restoring) and hydrodynamic reactions. The hydrostatics are most strongly nonlinear and are calculated using a ship hydrostatics computer program. In order that the zeroth-order solutions are expressed in terms of known analytic functions, the restoring moment curve needs to be fitted by a cubic polynomial. Although this fit may be somewhat approximate for the MOB SBU case, it is assumed that it will yield at

PHILOSOPHICAL TRANSACTIONS OF THE ROYAL SOCIETY A MATHEMATICAL, PHYSICAL & ENGINEERING SCIENCES

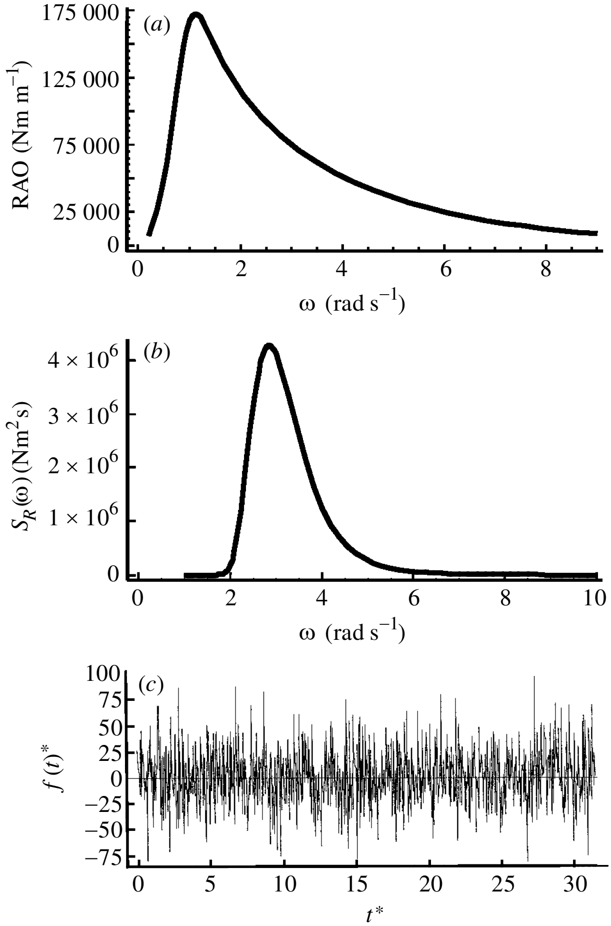

Figure 1. (*a*) *Patti-B* roll-moment excitation transfer function (RAO). (*b*) *Patti-B* roll-moment excitation spectrum ($U_{\mathrm{w}} = 2.75\ \mathrm{m\,s^{-1}}$). (*c*) *Patti-B* corresponding roll-moment excitation time history.

least the correct qualitative behaviour. It should be noted here that it is not much more difficult to use a numerically generated zeroth-order solution which is based upon an accurate higher-order righting-arm curve (Zhang & Falzarano 1994). The hydrodynamic part of the reactive force is that due to the so-called radiated wave force. The radiated wave force is subdivided into added mass (inertia) and radiated wave damping. These two forces are also strongly a function of frequency. However, since the damping is light, and for simplicity, constant values at a fixed frequency are assumed. Generally, an empirically determined nonlinear viscous damping term is included. However, such empirical viscous damping results are only available for ship hulls. The resulting equation of motion is

$$(I_{44} + A_{44}(\omega_n))\ddot{\phi} + B_{44}(\omega_n)\dot{\phi} + B_{44\mathrm{q}}\dot{\phi}|\dot{\phi}| + \Delta GZ(\phi) = F(t). \tag{2.1}$$

The focus of this study is nonlinear ship and floating offshore platform rolling motion in a realistic seaway due to a pseudo-random wave excitation. The effect

PHILOSOPHICAL TRANSACTIONS OF THE ROYAL SOCIETY A MATHEMATICAL, PHYSICAL & ENGINEERING SCIENCES

of seaway intensity is accurately considered. In order to obtain the roll-moment excitation spectrum, the sea spectrum is multiplied by the roll-moment excitation response amplitude operator (RAO) squared (see equation (2.2 *a*)). The RAO for the small fishing vessel in given in figure 1*a*.

The sea spectral model used for the small fishing vessel is the Pierson–Moskowitz (PM). The PM sea-state equation (Ochi 1998) is as follows:

$$S^{+}(\omega)=\frac{8.1\times10^{-3}g^{2}}{\omega^{5}}\mathrm{e}^{-0.74(g/U_{\mathrm{w}}\omega)^{4}},$$

where U_{w} is the wind speed. The PM model is used for this case because it corresponds to a fully developed seaway, which is in some sense the most severe. Moreover, the spectrum is a one-parameter spectrum so that solely the effect of seaway intensity can be considered.

The sea spectral model used for the SBU of the MOB is the NATO sea-state descriptions, which use the Bretschneider sea-state formula. The Bretschneider sea-state formula (Ochi 1998) is expressed as

$$S^{+}(\omega)=0.1687H_{\mathrm{s}}^{2}\frac{\omega_{\mathrm{s}}^{4}}{\omega^{5}}\mathrm{e}^{-0.675\omega_{\mathrm{s}}^{4}/\omega^{4}},$$

where H_{s} is the significant wave height (i.e. the average of the one-third highest waves) and ω_{s} is the significant wave frequency. The NATO model is used because it corresponds to a typical random seaway encountered in the North Atlantic operating areas of the NATO navies. In general, the Bretschneider sea spectrum is a two-parameter seaway with significant wave height and significant period as the two parameters. However, using the NATO wave data, the seaway intensity or sea-state number becomes the single parameter.

These two sea spectral formulae are based upon limited theoretical analysis and extensive wave data analysis. Various additional relationships can be derived by manipulating these formulae and applying the Rayleigh PDF (Ochi 1998).

Figure 1*b*, *c* shows the excitation spectra for the *Patti-B* and the corresponding time history of the forcing (in non-dimensional form) for a wind speed of $U_{\mathrm{w}}=2.75\ \mathrm{m\,s^{-1}}$. Figure 2 is for larger U_{w}. The significant wave heights for the sea spectra used for the *Patti-B* range from less than 0.6 m to almost 2.3 m. Although a different sea-state formula is used for the MOB, in order to relate the two vessels, the sea-state intensity ranges from about sea state 1 to 4 (Bhattachrayya 1978) for the *Patti-B* and sea states 5 to 9 for the MOB. Alternatively, the seaways considered for the MOB have significant wave heights, which range from *ca.* 3.2 m to 13.8 m.

It should also be noted herein that the complicated MOB roll-response RAO calculated was approximated by the smooth curve depicted in figure 3*a*. However, the true RAO calculated exhibited numerous humps and hollows at higher frequencies beyond the peak. Due to the small amount of wave energy at these frequencies, these oscillations were ignored. The resulting excitation spectrum is decomposed into periodic components with random phase angles. The time-dependent forcing function would then assume the form shown in figure 3*c*:

$$S_{\mathrm{R}}^{+}(\omega)=|\mathrm{RAO}|^{2}S^{+}(\omega), \tag{2.2 a}$$

$$F(t)=\sum_{i=1}^{N}F_{\mathrm{M}}(\omega_i)\cos(\omega_i t+\gamma_i), \tag{2.2 b}$$

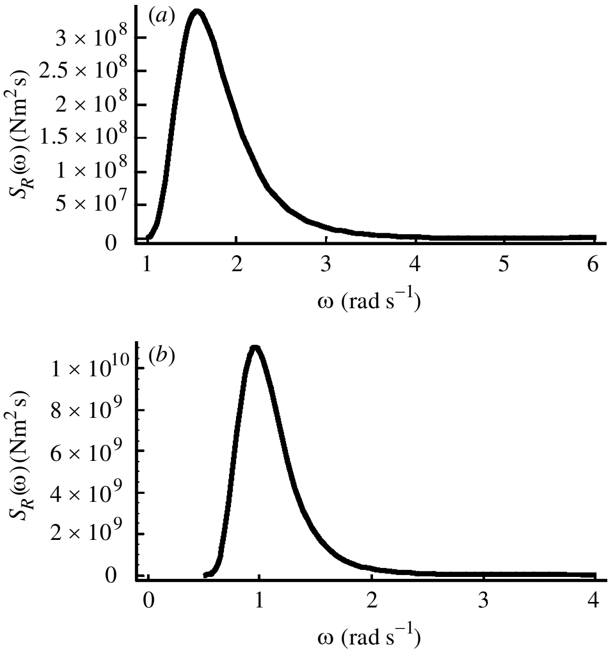

Figure 2. (*a*) *Patti-B* moderate-amplitude roll-moment excitation spectrum ($U_w = 5.15$ m s^{-1}). (*b*) *Patti-B* large-amplitude roll-moment excitation spectrum ($U_w = 10.0$ m s^{-1}).

where

$$F_M(\omega_i) = \sqrt{2S_R^+(\omega_i)\Delta\omega}. \tag{2.2 c}$$

Figure 3*b*, *c* shows the MOB SBU excitation spectra and the corresponding time-dependent force (in non-dimensional form) for a NATO sea state 5. Figure 4 is the MOB excitation spectrum for sea state 9.

3. The dynamical perturbation method

The focus of this investigation is the extension of an approach previously used to study the nonlinear dynamics of a small fishing vessel and a very large semi-submersible platform due to pseudo-random wave excitation (Vishnubhotla *et al*. 1998, 1999). The approach was originally developed by Vakakis (1993, 1994) to calculate in closed form the homoclinic manifolds due to rapidly varying periodic excitation. That approach was generalized to calculate heteroclinic manifolds due to pseudo-random wave excitation. Considering that random excitation is a realistic model for ship and floating offshore platform motions at sea, this method was extended and then applied to consider the case of perturbed heteroclinic manifolds due to an external excitation as approximated by a finite summation of regular (periodic) wave components.

The solution to equations such as (2.1) with softening spring characteristics exhibits two greatly different types of motions depending upon the amplitude of the forcing. For small forcing amplitude, the first type of motion is an oscillatory motion

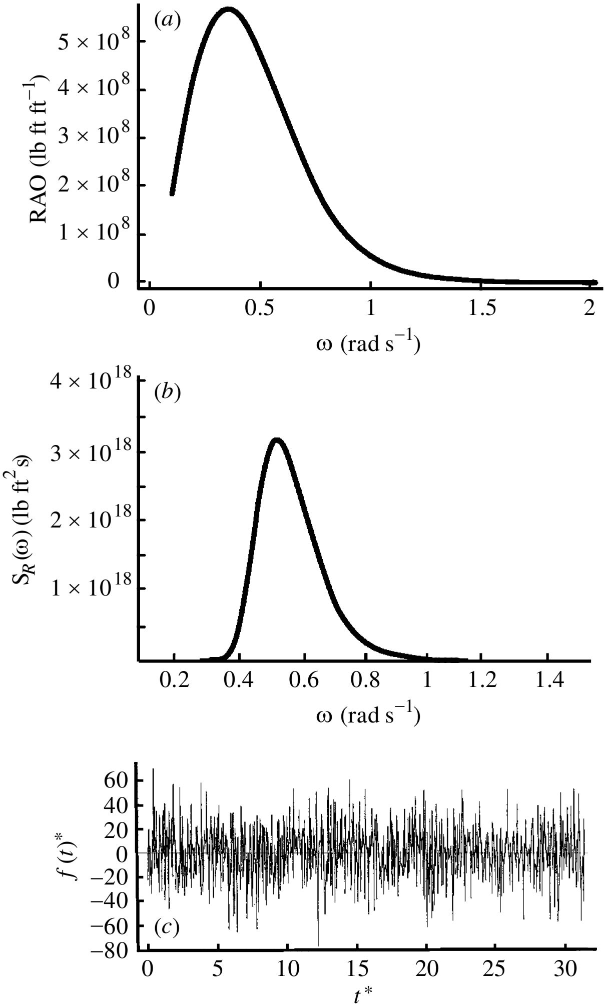

Figure 3. (*a*) MOB roll-moment excitation transfer function (RAO) (smoothed). (*b*) MOB roll-moment excitation spectra (NATO sea state 5) for $[H_s, T_0] = [10.7, 9.7]$. (*c*) MOB corresponding roll-moment excitation time history. Roll-moment excitation force (non-dimensionalized) for $[H_s, T_0] = [10.7, 9.7]$.

which is bounded and well behaved. For large amplitudes of forcing, the motion can be such that a unidirectional rotation occurs. The boundary between these two types of motions is called, in the terminology of nonlinear vibrations, the separatrix. This curve literally separates the two qualitatively different motions. In the language of nonlinear dynamical systems, these curves are called the (upper and lower) saddle connections. The saddles are connected as long as no damping and forcing are considered in the system. Once damping is added to the system, the saddle connection breaks into stable and unstable manifolds. The stable manifolds are most important because they form the basin boundary between initial conditions which remain bounded and those that become unbounded. When periodic forcing is added to the system, these manifolds oscillate periodically with time but return to their initial

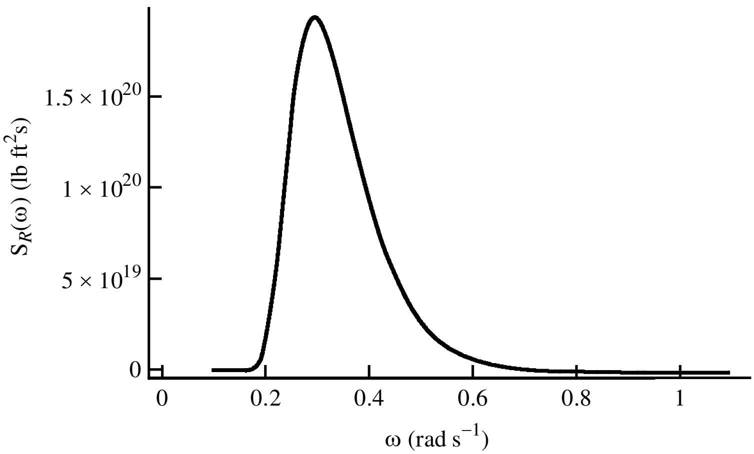

Figure 4. MOB large-amplitude roll-moment spectrum (NATO sea state 9). Roll-moment excitation spectra for $[H_{\rm s}, T_0] = [45.9, 20.0]$.

configuration after one period of the forcing. This forcing period is chosen for the Poincaré sampling time of such a periodic system. However, no such obvious Poincaré time sampling exists for the pseudo-randomly forced system studied herein.

In this investigation, the random wave forcing is approximated by a summation of periodic components with random relative phase angles. Although this representation approximates the true random excitation as $N \to \infty$ and $\Delta\omega \to 0$, for finite N this does not occur. Actually, the 'random' signal repeats itself after $T_{\rm R} = 2\pi/\Delta\omega$. Another relevant time period is the average or zero crossing period T_0. Assuming the spectra is narrow banded, this might also be a good reference period for a Poincaré map. In lieu of Poincaré maps, we choose to trace out single solution paths which are contained in the stable manifolds (see figure 5). These are then projected onto the phase plane.

The solutions lying in the stable manifolds are calculated using the new approach. This method is a perturbation method which begins with the undamped and unforced separatrix (see figure 5) which, for a simple softening spring (equation (3.1)), is known in closed form, i.e.

$$\ddot{x} + x - kx^3 = 0, \tag{3.1}$$

$$x(\tau) = \frac{1}{\sqrt{k}} \tanh\left(\frac{\tau - \tau_0}{\sqrt{2}} + \tfrac{1}{2}\right), \tag{3.2 a}$$

$$\dot{x}(\tau) = \frac{1}{\sqrt{2k}} \operatorname{sech}^2\left(\frac{\tau - \tau_0}{\sqrt{2}} + \tfrac{1}{2}\right), \tag{3.2 b}$$

where τ is the scaled time and τ_0 is the scaled initial time. The first-order solution is determined by using the method of variation of parameters. Equation (2.1) can now be scaled into the following form:

$$\ddot{x} + x - kx^3 = \epsilon(-\gamma\dot{x} - \gamma_{\rm q}\dot{x}|\dot{x}| + F(\eta)), \tag{3.3}$$

where $\eta = (\tau - \tau_0)/\sqrt{2} + \frac{1}{2}$. The solution method involves expanding the solution in a perturbation series as

$$x(\eta) = x_0(\eta) + \epsilon x_1(\eta) + \cdots . \tag{3.4}$$

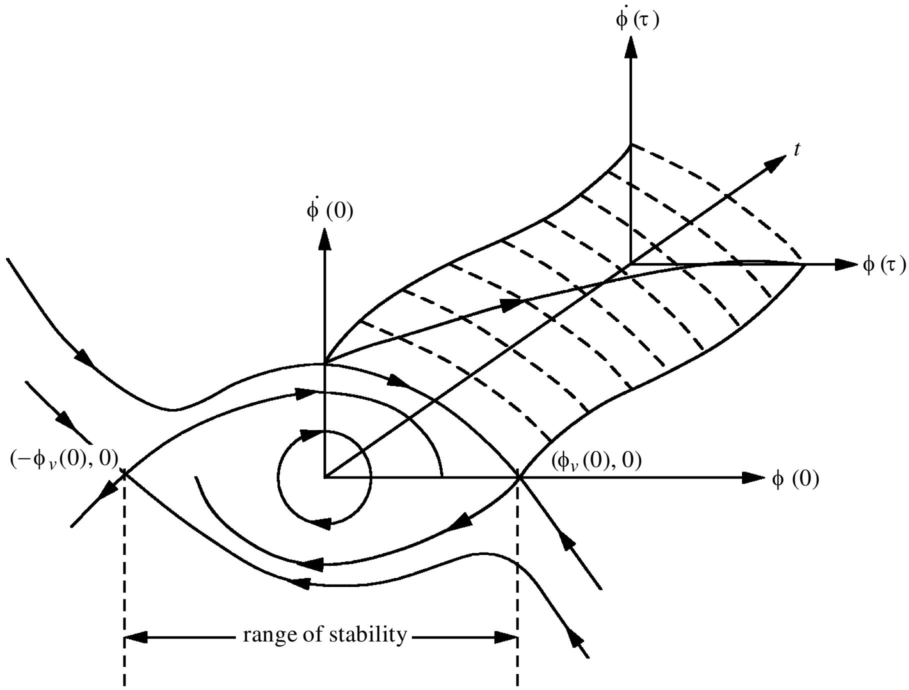

Figure 5. Extended phase space showing stable manifold and contained time-varying solution.

The first-order equation to be solved is actually a linear equation with time varying coefficients. The coefficients are obtained from the zeroth-order solution known from (3.1) and (3.2), i.e.

$$\ddot{x}_1 + x_1 - 3kx_1x_0^2 = \hat{G}(x_0, \eta, \tau_0). \tag{3.5}$$

Once the homogeneous solution is determined, the particular solution is then obtained by again using the technique of variation of parameters. The above first-order differential equation (3.5) is linear with non-constant coefficients and an inhomogeneous right-hand side $\hat{G}$. The non-constant coefficients and the right-hand side are composed of functions involving the now known zeroth-order solution and other known functions of time. The method is then used to determine the critical solutions which separate the bounded steady-state oscillatory motions from the unbounded motions. These solutions are determined by placing conditions on the varied parameters which multiply the homogeneous solutions.

The details of the solution procedure can be summarized as follows. To start, note that one of the first-order homogeneous solutions, $x_{\mathrm{h1}}^{(1)}$, is just the time derivative of the zeroth-order solution. The other first-order homogeneous solution, $x_{\mathrm{h1}}^{(2)}$, can then be obtained by applying the method of variation of parameters and using the Wronskian determinant. Once both homogeneous solutions are known, the particular solutions can be obtained by again applying the method of variation of parameters. The total solution given in (3.6) is then attainable from the summation of the homogeneous and particular parts. The only aspect that remains is to determine the values of the variation constants, α and β. These values are determined such that the stable solution remains bounded for all positive time to infinity while the unstable solution remains bounded for all negative time to infinity.

Vakakis originally developed this technique to study the Holmes–Duffing (buckled beam) oscillator with a rapidly varying external excitation and the details of that analysis are described in Vakakis (1993). The approach taken in this paper, although different from the original analysis, is similar enough that all the details need not be completely repeated herein. The first-order solution for the perturbed manifolds is as follows:

$$x_1(\eta) = x_{\mathrm{h1}}^{(1)}(\eta)\left(\alpha - \int_0^{\eta} x_{\mathrm{h1}}^{(2)}(\tau)\hat{G}(\tau)\,\mathrm{d}\tau\right) + x_{\mathrm{h1}}^{(2)}(\eta)\left(\beta - \int_0^{\eta} x_{\mathrm{h1}}^{(1)}(\tau)\hat{G}(\tau)\,\mathrm{d}\tau\right). \tag{3.6}$$

The associated constants (the varied parameters) are determined such that the critical basin boundary solutions remain bounded for infinite time (Vakakis 1993). These conditions provide the stable and unstable manifolds associated with the positive and negative angles of vanishing stability and correspond to the upper and lower separatrices, respectively. The stable manifolds form the basin boundary between bounded (safe non-capsizing) and unbounded (capsizing) solutions (see, for example, figure 5). It is also possible to determine the unstable manifolds by choosing the variation constants such that the manifolds remain bounded for minus infinite time. The unstable manifolds are important because they interact with the stable manifolds and erode the safe basin. The integrals in (3.6) can be determined analytically in series form for simple springs and numerically for more complicated springs. This is the key aspect of the method in that it is capable of yielding exact series solutions for simple springs which later can be used to verify approximate numerical results.

Although this method was originally developed by Vakakis (1993) to study intersections of stable and unstable manifolds for equations for which the Melnikov method could not be used, this method is applied herein because it is general enough to yield exact solutions to general equations such as the multiple frequency forcing case being studied. This multiple frequency forcing case is an engineering approximation used in time domain simulations and physical scale model testing in wave tanks to model a truly random seaway which occurs in nature. However, each time history represents a single realization of the random seaway. In order for the results of such an investigation to be useful, multiple realizations must be considered. One must then obtain average and standard deviation values of the manifold locations. Whether or not the pseudo-random representation of the spectra is a valid random representation is an extensively debated subject in naval architecture and offshore engineering (Chakrabarti 1989). Although, for finite N, this representation does not satisfy the condition of a Gaussian seaway or response, it does so in the limit as $N \to \infty$. Alternative representations of the random seaway do exist and include filtered white noise. However, this may not be easily applicable to the present problem.

4. Results

The results are for two vessels, which essentially span the entire size range of ships and floating offshore platforms, either existing or planned. The first set of results is for a small fishing vessel which is probably one of the smallest vessels to venture away from safety of shore. The second set of results is for an SBU of the US Navy's planned MOB. Alternatively, the MOB SBU, if built, will be the largest floating vessel ever built. The two sets of results are shown for comparison since they exhibit such qualitatively different types of behaviour. Even though the seaway intensities are different, with the *Patti-B* exposed to mild seaways and the MOB exposed to more severe seaways, the vessels' relative sizes are so vastly different that the results are still qualitatively different.

An indication of if the basin boundaries will be simple and smooth or fractal and complicated is determined by whether the manifolds intersect or not. As a first step in determining whether or not this will occur for the pseudo-randomly forced system, we determine solutions which lie in both the stable and unstable manifolds. After this is done, the distance between the two solutions can then be determined and this will indicate whether or not a manifold intersection has occurred. When the distance between the two manifolds goes to zero, the manifolds become tangent and this is a critical value of the forcing. Beyond the value of forcing where the manifolds become tangent, the manifolds intersect and the safe basin begins to erode. This is exactly what the Melnikov function (Falzarano *et al*. 1992) is used for and what is being developed herein is simply a more general alternative to the Melnikov approach. The method described has several potential benefits over the classical Melnikov approach. These benefits enable us to (a) analyse very general systems for which the Melnikov method is not valid, (b) obtain higher-order results, and (c) develop a visual projection of the manifolds for single-degree-of-freedom systems.

(*a*) *Patti-B safe basin boundary projected phase plane*

The first set of results is for physical parameters representing the clam dredge *Patti-B* (Falzarano *et al*. 1992) in beam seas and rolling in various intensity PM sea spectra. As stated previously, the sea spectra are approximated by a finite but large number of periodic components. As can be seen, when the wind speed is increased and the seaway intensity increases, the vessel's dynamics change qualitatively. The upper and lower stable manifolds change from smooth curves similar to the unforced system to rather complicated curves indicating the possibility of manifold intersections. The size of the safe operating region of the vessel is somewhat related to when these manifolds intersect and become fractal or complicated. Figure 2 shows moderate- and large-amplitude sea spectra plotted against frequency for a range of wind speeds. The wind speed is the single parameter describing the seaway intensity. Results for time-varying roll-motion solutions contained within the upper and lower stable manifolds projected phase planes for these sea spectra are given in figure 6. When looking at these projected phase-plane results, it should be recognized that the solutions depicted represent a time evolution of a single trajectory and are not Poincaré time samplings of the manifold. This explains the wrapping around the fixed point. The random oscillation occurs on the average at the zero crossing period while the solution is slowly evolving towards the fixed point.

(*b*) *MOB safe basin boundary projected phase plane*

The second set of results is for parameters representing the USNA generic MOB hull-form at transit draft in beam seas rolling in various intensity NATO sea spectra. As stated previously, the sea spectra are approximated by a finite number of

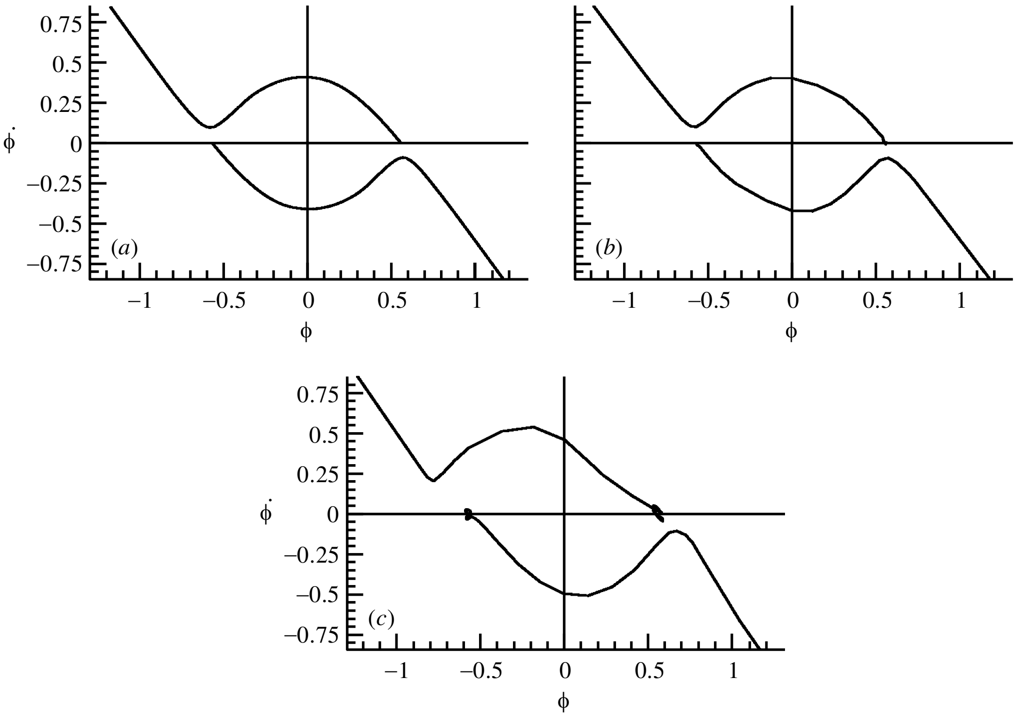

Figure 6. (a) *Patti-B* projected phase plane for PM spectra ($U_{\mathrm{w}} = 2.75\ \mathrm{m\,s^{-1}}$). ($b$) *Patti-B* projected phase plane for PM spectra ($U_{\mathrm{w}} = 5.15\ \mathrm{m\,s^{-1}}$). ($c$) *Patti-B* projected phase plane for PM spectra ($U_{\mathrm{w}} = 10.0\ \mathrm{m\,s^{-1}}$).

periodic components. As can be seen, when the seaway intensity increases, the vessel's dynamics change qualitatively. The distance between the upper and lower stable manifolds and the roll axis in the neighbourhood of the angle of vanishing stability changes as the intensity of the seaway increases. As the wave amplitude increases, the magnitude of the unstable periodic orbit in the neighbourhood of the angle of vanishing stability increases. In our previous analysis of a small fishing vessel above, the manifolds changed from smooth curves similar to the unforced system to rather complicated curves, indicating the possible presence of manifold intersections. Since the MOB is so large, these rather severe seaways do not dramatically affect the manifolds.

Figure 3b, c shows moderate- and large-amplitude Bretschneider sea spectra plotted versus frequency for sea-state intensities 5 and 9, with the sea-state intensity being the variable parameter. The projected phase planes results for time-varying roll-motion solutions contained within the upper and lower stable manifolds are given in figure 7. It should be noted that the results given are non-dimensionalized, using the non-dimensionalization implied by (3.3).

(c) *Patti-B extended state-space results*

Once unstable manifolds are included, the two-dimensional projection of the time-varying solutions which lie in the stable or unstable manifolds may be deceptive. This is so because true intersections only occur for the same time phase. Therefore, a three-

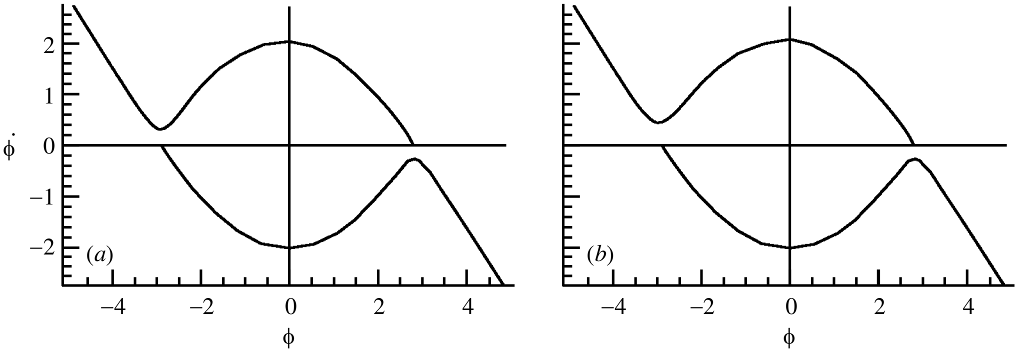

Figure 7. MOB projected phase plane for NATO sea spectra: (*a*) sea state 5 (for $[H_s, T_0] = [10.7, 9.7]$); (*b*) sea state 9 (for $[H_s, T_0] = [45.9, 20.0]$).

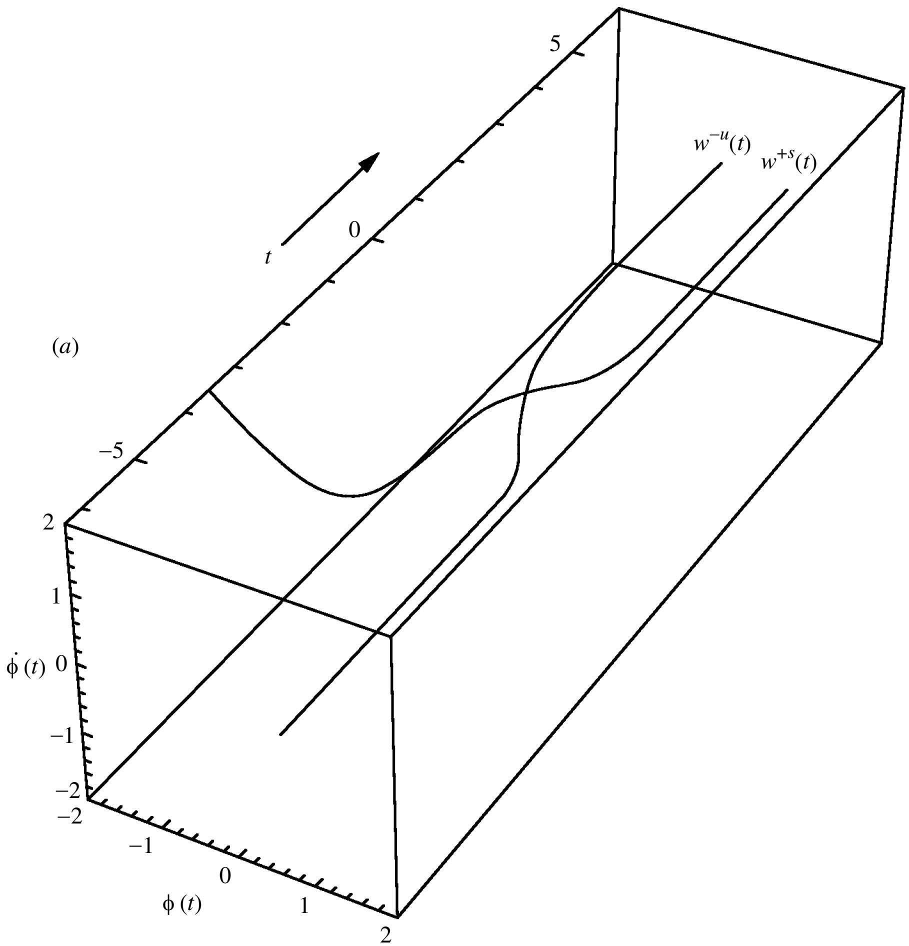

Figure 8. *Patti-B* extended phase space showing solutions contained in stable and unstable manifold ($U_w = 2.75$ m s^{-1}, $V = 2.75$ m s^{-1}).

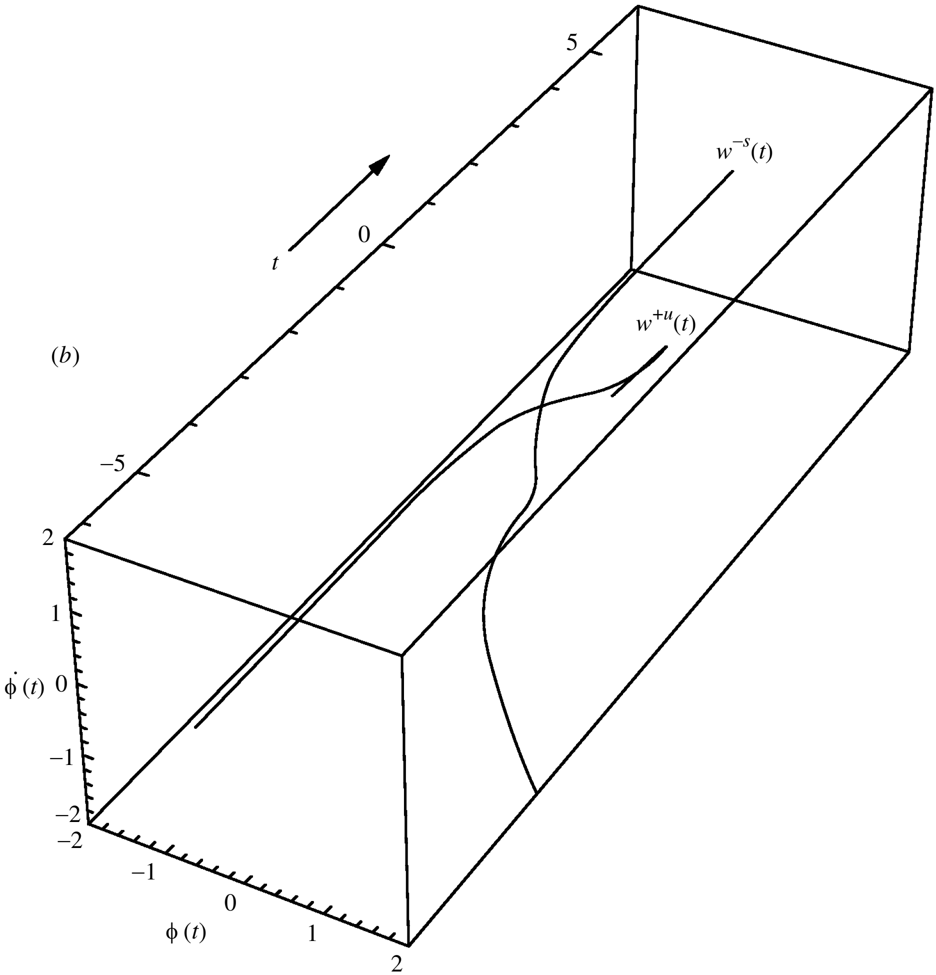

Figure 8. (*Cont.*)

dimensional extended state-space representation is the only unique representation. In order to illustrate this, and in order to determine whether or not intersections have occurred, some typical results for the *Patti-B* are provided. These one-dimensional solution curves are displayed in the full three-dimensional extended state space (figure 8). These results clearly indicate that the two curves do not intersect for the two given seaway intensities. A more extensive and systematic investigation is currently underway. In order to determine more clearly if the manifolds' intersections have occurred, the entire manifold must be generated. Generating the entire manifold would involve varying the initial time t_0 and then generating an entire manifold mesh. After this had been done, the distance between the two manifolds, i.e. stable and unstable, can then be calculated. This distance going to zero would indicate that manifold intersections were imminent. This would be a critical value of external wave forcing since, at a greater value of wave forcing, the safe basin would begin to erode.

5. Conclusions

The described method is quite powerful and capable of handling very general systems. The application herein used the knowledge of the zeroth-order solution, which was known in closed form for this simple system. However, this is not a requirement and actually for more general systems it could be known numerically. Clearly, the safe operating region of the vessel is directly related to when the calculated stable and unstable manifolds intersect and erode the safe basin. It should be re-emphasized here that the results given correspond to single realizations of the given sea spectra. In order to gain a more complete probabilistic understanding of the system's random behaviour, multiple realizations must be considered and analysed. This ensemble of results should then be analysed in terms of averages and standard deviations. However, this has not yet been done in a systematic manner.

The results clearly demonstrate the effect of random excitation on the global non-linear dynamics of both vessels about their roll axes. However, it should be noted again that, in general, for typical semi-submersibles, the roll axis is not the critical rotation axis. The critical axis is often an approximately diagonal axis (Kota *et al.* 1998). It is believed that due to the large length-to-beam ratio of the MOB SBUs, the roll axis is most probably the critical axis or quite close to the critical axis.

J.F. acknowledges the support of the Office of Naval Research MOB S&T Project and its program manager Gene Remmers and the NFESC MOB Project Team. J.F. and A.V. also acknowledge the support of the US National Science Foundation, Dynamical Systems and Control Program for their past and present support of this and related work.

References

Bhattachrayya, R. 1978 *Dynamics of marine vehicles*. Wiley.

Chakrabarti, S. K. 1989 *Hydrodynamics of offshore structures*. Springer.

Falzarano, J., Shaw, S. & Troesch, A. 1992 Application of global methods for analyzing dynamical systems to ship rolling motion and capsizing. *Int. J. Bifurcation Chaos* **2**, 101–115.

Hsieh, H., Shaw, S. & Troesch, A. 1993 A predictive method for vessel capsize in a random seaway. In *Nonlinear dynamics of marine vehicles* (ed. J. Falzarano & F. Papoulias), pp. 103–123. ASME.

Kota, R., Falzarano, J. & Vakakis, A. 1997 *ISOPE Conf*, pp. 492–498.

Kota, R., Falzarano, J. & Vakakis, A. 1998 Survival analysis of deep-water floating offshore platform about its critical axis: including coupling. *J. Int. Soc. Offshore Polar Engineers* **8**, 115–121.

Lin, H. & Yim, S. 1995 Chaotic roll motion and capsizing of ships under periodic excitation with random noise. *Appl. Ocean Res.* **117**, 185–204.

National Transportation Safety Board (NTSB) 1979 Grounding and capsizing of the clam dredge *Patti-B*. NTSB Marine Accident Report.

Newman, J. 1982 *Marine hydrodynamics*. Cambridge, MA: MIT Press.

Ochi, M. 1998 *Ocean waves*. Cambridge University Press.

Simiu, E. & Frey, M. 1996 Melnikov processes and noise induced exits from potential well. *J. Engng Mech.* **122**, 263–270.

Soliman, M. & Thompson, J. M. T. 1990 Stochastic penetration of smooth and fractal basin boundaries under noise excitation. *Dynamics Stability Systems* **5**, 281–298.

Thompson, J. M. T. 1997 Designing against capsize in beams seas: recent advances and new insight. *Appl. Mech. Rev.* **6**, 307–325.

Vakakis, A. 1993 Splitting of separatrices of the rapidly forced Duffing equation. *Nonlinear Vibrations* (September), pp. 249–255.

Vakakis, A. 1994 Exponentially small splitting of manifolds in a rapidly forced Duffing system. *J. Sound Vib.* **170**, 119–129.

Vishnubhotla, S., Falzarano, J. & Vakakis, A. 1998 A new method to predict vessel/platform capsizing in a random seaway. In *Third Int. Conf. on Computational Stochastic Mechanics*, pp. 497–502. Rotterdam: Balkema.

Vishnubhotla, S., Falzarano, J. & Vakakis, A. 1999 Mobile offshore base (MOB) dynamics in a random seaway. In *Int. Soc. of Offshore and Polar Engineers Conf., May–June*, pp. 531–535.

Webster, W. 1989 The transverse motions. Seakeeping. In *Principles of naval architecture*, ch. 8, vol. III, pp. 73–88. New York: Society of Naval Architects and Marine Engineers.

Zhang, F. & Falzarano, J. 1994 Multiple degree of freedom global transient ship rolling motion: large amplitude forcing. In *Stochastic dynamics and reliability of nonlinear ocean systems*, pp. 99–108. ASME.